



Molecular Docking and In Vitro Studies of Synthesized Oxadiazole Derivatives as Urease Inhibitors

Kamran Mehdi^{1,2}, Obaid-ur-Rahman Abid², Saqib Khan¹, Is Helianti³,
Muhammad Ikhlas Abdjan⁴, Aleesha Aleesha¹, Muhammad Ali¹ &
Naseer Ahmed^{3*}

¹Department of Chemistry Government Postgraduate College Haripur, Affiliated with University of Haripur, GT Road Haripur, 22620, Pakistan

²Department of Chemistry, Hazara University Mansehra, Mansehra, 21300, Pakistan

³Research Centre for Genetic Engineering, Research Organization of Life Sciences and Environment, National Research and Innovation Agency-Republic of Indonesia (BRIN), KST Soekarno, Jalan Raya Bogor Km 46, Cibinong, Bogor, West Java 16911, Indonesia

⁴Department of Chemistry, Faculty of Mathematics and Natural Science, Universitas Negeri Surabaya, Jalan Ketintang Wiyata No.62, Surabaya, 60231, Indonesia

*E-mail: nase001@brin.go.id

Abstract. A novel sequence of 1,3,4-oxadiazoles (7a–h) was synthesized. The compounds were characterized by IR, ¹H NMR, and MS analyses. They were also examined to determine whether they could prevent urease from functioning. Molecular docking was done with AutoDock Vina, and the findings were visualized in Discovery Studio. The H NMR spectra showed peaks at δ 10.20 to 10.69 ppm for NH protons, δ 7.16 to 8.01 ppm for aromatic protons, and δ 4.21 to 4.37 ppm for 2H and CH₂ groups, confirming the structural details. The EI-MS spectra showed molecular ion peaks at 337 m/z with an intensity of 14-67%. Among the bioactivity-tested compounds, 7d resulted in robust activity with IC₅₀ values of $161.6 \pm 5.8 \mu\text{M}$; compound 7e exhibited the weakest activity, at $453.6 \pm 5.8 \mu\text{M}$; and no inhibition was discovered by the 7a, 7f, and 7h compounds when compared to the Thiourea, at $21.8 \pm 1.51 \mu\text{M}$. Molecular dockings confirmed compound 7d as the best-docked complex, with a minimum energy of -7.4 kcal/mol, an RMSD value of 1.573 Å, and hydrogen interactions at His593 with the active site residue, confirming the experimental results. It was determined that 1,3,4-oxadiazoles can be employed as urease inhibitors.

Keywords: *AutoDock Vina; characterization; in vitro study; molecular docking; oxadiazoles; urease inhibition.*

1 Introduction

Urease functions as a nickel-dependent metalloenzyme broadly distributed among bacteria, plants, fungi, and algae [1]. It was the first enzyme to be crystallized in 1926 by Sumner [2]. After its discovery in plants [3], the urease of *Canavalia ensiformis* (Fabaceae) has been thoroughly studied. The chemical composition of urease from *Klebsiella aerogenes* was initially described in 1995

[4] and jack bean urease has been key in understanding its function [5]. Urease's primary role is to help organisms grow by providing nitrogen in the form of ammonia [6]. However, this reaction leads to a rapid increase in pH due to the accumulation of ammonia, resulting in several adverse effects in agriculture and medicine [7]. In soil, the activity of urease contributes to ammonia toxicity, loss of nitrogen as gas, damage to young plants, and reduced efficiency of nitrogen uptake, undermining the benefits of urea fertilizers [8].

In clinical settings, urease-producing bacteria, such as *Helicobacter pylori*, are implicated in serious health conditions, including gastroduodenal ulcers, gastric cancer, urolithiasis, and urinary catheter encrustation [9]. Other diseases associated with urease activity include hepatic encephalopathy, pyelonephritis, and the formation of kidney stones [10]. As a result, urease inhibition has become a hot topic in the last few years, leading to the discovery of numerous anti urease agents [11]. Notable examples include hydroxamic acid derivatives [12], hydroxyurea [13], hydroxamic acids [14], phosphorodiamidates [15]. Whereas Hydroxamic acids are potent but metals ions can cause teratogenicity in rats [16]. Schiff-based metal ion complexes block urease, however, because of heavy metal atoms, it is harmful for human health, rendering them inappropriate for medicinal application [17]. Metal-based inhibitors, such as those involving nanoparticles and other metals, including silver, copper, nickel, and zinc, are also effective, but come with drawbacks like potential toxicity, environmental concerns, and the possibility of developing resistance.

A stronger and less hazardous source that can efficiently inhibit urease is required due to the shortcomings of the existing inhibitors. Urease inhibitors are thought to be important therapeutic medications for managing infections brought on by these pathogens and preventing associated effects [18]. Urease facilitates the rapid breakdown of urea-based fertilizers in soil, causing ammonia volatilization. This process results in significant nitrogen loss, reduced fertilizer efficacy, and environmental pollution. Urea hydrolysis is slowed down by urease inhibitors, which enhances agricultural yield, ecological sustainability, and the efficiency of nitrogen absorption. The discovery of 1,3,4-oxadiazole derivatives as a potential urease inhibitor has led to the development of new drugs for use in agriculture and medicine. Potential uses for environmentally friendly farming and prevention of infections might arise from continual optimization and evaluation [19].

Oxadiazole derivatives are known for their non-toxic nature and potential use as drugs. Oxadiazole derivatives are considered the best inhibitors against urease [20]. An example is 5-(4-chlorobenzyl)-1,3,4-oxadiazole-2(3H)-thione, which is twenty times more active than the standard inhibitor [21]. Oxadiazole is a significant heterocyclic compound that is composed of five-membered rings and contains one oxygen and two nitrogen elements [22], which is thought to be

produced from furan by substituting two pyridine-type nitrogen (-N=) groups for two methane (-CH=) groups [23]. However, due to its several significant chemical and biological characteristics, 1,3,4-oxadiazole is the most well-known and extensively researched by scientists [24]. This study focused on the synthesis of new urease inhibitors, with particular attention to 1,3,4-oxadiazoles, starting from the synthesized 1,4-disubstituted thiosemicarbazides. This was then converted into oxadiazoles by reacting them with mercuric acetate in methanol. The synthesized compounds were characterized using various spectroscopy methods. After evaluation of the compound's urease inhibition activity, their interactions with urease were checked by performing molecular docking.

2 Materials and Method

2.1 Chemicals and Instruments

For the synthesis of a 1,3,4-oxadiazole derivative, the following materials and equipment are required: (a) concentrated H₂SO₄, dry CH₃OH, reflux; (b) conc. sulfuric acid; (c) Hg (OAc)₂; (d) reflux, pre-coated silica gel GF-254 aluminum plates (Kieselgel 60, 20, 0.5 mm thick, E. Merck, Germany), TLC was performed using dry methanol; (e) N₂H₄·H₂O (80%), dry CH₃OH, reflux. The same pre-coated TLC plates (silica gel) were used to test the samples' purity.

2.2 Substituted Esters 2(a-c) Synthesis

Methyl esters 2(a-c) were synthesized via esterification of substituted phenylacetic acids 1(a-c) with CH₃OH in the presence of catalytic amounts of concentrated H₂SO₄. In this procedure, 0.015 moles of the respective acids were dissolved in 20 mL of methanol in a round-bottom flask fitted with a reflux condenser and drying tube. A few drops of conc: H₂SO₄ were added to catalyse the reaction, which was then refluxed under continuous stirring for four hours. Reaction progress was continuously monitored using TLC. Upon completion, excess CH₃OH was removed by evaporation, and the resulting oily residue was transferred to a separating funnel containing water. Subsequently, 30 mL of CH₂Cl₂ was added for extraction. The unreacted acid was extracted using a sodium hydrogen carbonate solution. The organic component was separated and dehydrated using anhydrous CaCl₂. Evaporation eliminated the solvent, leaving behind only the ester. Characterization of the ester was then done using IR spectroscopy.

2.3 Substituted Hydrazides 3(a-c) Synthesis

After dissolving 0.012 moles of substituted ester in 20 mL of methanol, 0.015 moles of hydrazine hydrate were added drop by drop while being constantly

stirred. To produce the matching hydrazides, the mixture was refluxed and was stirred continuously for two to three hours. Reaction completion was confirmed by TLC. The resulting hydrazides (3a–c) were purified by recrystallization using aqueous C_2H_5OH .

2.4 1,4-disubstituted thiosemicarbazides (5a-h) Synthesis

The corresponding thiosemicarbazides (5a-h) were synthesized by treating 0.006 moles of carboxylic acid hydrazide with 0.006 moles of isothiocyanate. After dissolving the hydrazide in 15 to 20 mL of methanol and the isothiocyanate separately in 10 to 15 mL of methanol, the two solutions were mixed. Ten to twelve hours were spent refluxing the reaction mixture. TLC was employed to monitor reaction completion. After the reaction, the mixture was allowed to cool to room temperature. In order to obtain pure compounds, the resulting crude solid was recrystallized from aqueous ethanol.

2.5 1,3,4-Oxadiazoles 7(a-h) Synthesis

Thiosemicarbazides (0.001 moles) were cyclized to produce oxadiazole using $Hg(OAc)_2$ (0.001 moles) in 10 mL of CH_3OH as solvent. $(CH_3COOCH_2CH_2(C_6H_{14}))$ (3:7) was used as the mobile phase in TLC to track the reaction mixture's progress throughout a 6-hour reflux at 100 °C. To isolate the pure oxadiazole derivatives, cooling the reaction mixture and pouring it into cold water helped precipitation. The resulted precipitate was collected by filtration, washed thoroughly with water, and purified by recrystallization from ethanol. Because mercuric acetate is hazardous, all reactions involving it were carried out in a fume hood with adequate ventilation and PPE, such as a lab coat, safety goggles, and gloves. Waste containing mercury was managed and disposed of in accordance with accepted hazardous chemical procedures.

7a: 5-(2,3-dichlorobenzyl)-N-(2-fluorophenyl)-1,3,4-oxadiazol-2-amine

%Yield: 52, m.p. 264-266 °C; white crystalline solid, EI-MS m/z (rel. int. %): 337 (M^+ , 57), 226 (43), 302 (80), 110 (55), 159 (100), 83 (8); 1H NMR (DMSO-d6, 300 MHz); 8.00 (t, J =8.1 Hz, 1H , Ar), δ 10.21 (s, 1H), 7.62 (d, J =8.1 Hz, 1H , Ar), 7.40 (d, J =7.8, 1H , Ar), 7.47 (d, J =6.6, 1H, Ar), 7.27-7.16 (m, 2H, Ar), 4.35 (s, 2H, CH_2), 7.08-7.02 (m, 1H, Ar).

7b: 5-(2,3-dichlorobenzyl)-N-(3-fluorophenyl)-1,3,4-oxadiazol-2-amine

%Yield: 58, m.p. 271-273 °C, white solid; EI-MS m/z (rel. int. %): 337 (M^+ , 34), 227 (47), 302 (77), 123 (58), 159 (100), 95 (73); 1H NMR (DMSO-d6, 300 MHz); δ 10.69 (s, 1H , NH), J = 8.1 Hz. = 8.1 HzH, Ar), 7.62 (d, J = 7.2 Hz = 7.2 Hz, 7.48 (d, J =8.1Hz, 1H , Ar), 7.25 (d, J =8.1Hz, 1H, Ar), 7.42-7.30 (m, 3H, Ar), 4.37 (s, 2H, CH_2), 6.79 (dt, J =8.4, 1.5Hz, 1H , Ar).

7c: 5-(2,3-dichlorobenzyl)-N-(4-fluorophenyl)-1,3,4-oxadiazol-2-amine

%Yield: 64, m.p. 267-269 °C, white solid; EI-MS m/z (rel. int. %): 337 (M⁺, 67), 226 (55), 302 (70), 110 (68), 159(100), 83(77); ¹H-NMR (DMSO-d6, 300 MHz); δ 10.43 (s, ¹H, NH), 7.19-7.13 (m, 2H, Ar), 4.35(s,2H, CH2), 7.55-7.46 (m, 3H, Ar), 7.62 (d, J=7.2Hz, 1H, Ar), 7.38 (d, J=7.2Hz, ¹H, Ar).

7d: 5-(2,4-dichlorobenzyl)-N-(2-fluorophenyl)-1,3,4-oxadiazol-2-amine

%Yield: 47, m.p. 259-262 °C, white solid; EI-MS m/z (rel. int. %): 337 (M⁺, 60), 110 (49), 159 (100), 83(85); ¹H NMR (DMSO-d6, 300 MHz); δ 10.20 (s, ¹H, NH), 7.65 (bs, 1H, Ar), 8.01 (t, J=8.1Hz, 1H, Ar), 7.63 (d, J=8.4Hz, ¹H, Ar), 7.27-7.16 (m, 2H, Ar), 7.33 (dd, J=8.1, 1.5Hz, 1H, Ar), 4.22 (s, 2H, CH2), 7.08-7.04 (m, ¹H, Ar).

7e: 5-(2,4-dichlorobenzyl)-N-(3-fluorophenyl)-1,3,4-oxadiazol-2-amine

%Yield: 59, m.p. 256-257 °C, white solid; EI-MS m/z (rel. int. %): 337 (M⁺, 52), 159 (100), 302 (59), 95 (78), 111(62); ¹H-NMR (DMSO-d6, 300 MHz); δ 10.69 (s,1H, NH), 7.51-7.24 (m, 5H, Ar), 7.68 (d, J=1.8Hz, 1H, Ar), 6.79 (dt, J=8.4, 4.29 (s, 2H, CH2), 1.8Hz, ¹H, Ar).

7f: 5-(2,4-dichlorobenzyl)-N-(4-fluorophenyl)-1,3,4-oxadiazol-2-amine

%Yield: 62, m.p. 277-279 °C, white crystalline solid; EI-MS m/z (rel. int. %): 337 (M⁺, 14), 159 (100), 301 (22), 123(38), 57(88), 82 (66); ¹H NMR (DMSO-d6, 300 MHz); 7.66 (d, J=1.2Hz, ¹H, Ar), δ 10.43 (s, 1H, NH), 77.16 (t, J=9.0, 2H, Ar), .55- 7.43 (m, 4H, Ar), 4.28 (s, 2H, CH₂).

7g: 5-(3,4-dichlorobenzyl)-N-(3-fluorophenyl)-1,3,4-oxadiazol-2-amine

%Yield: 67, m.p. 273-276 °C, white solid; EI-MS m/z (rel. int. %): 337 (M⁺, 42), 280 (30), 123(66), 159 (100), 95 (86); ¹H NMR (DMSO-d6, 300 MHz); 7.66 (s, ¹H, Ar), δ 10.68 (s, 1H, NH), 7.63 (d, J=8.4Hz, ¹H, Ar), ¹H, Ar), 7.35-7.24 (m, 3H, Ar), 7.45 (d, J=11.7Hz, 4.23 (s, 2H, CH2), 6.79 (dt, J=8.1, 1.8Hz, ¹H, Ar).

7h: 5-(3,4-dichlorobenzyl)-N-(4-fluorophenyl)-1,3,4-oxadiazol-2-amine

%Yield: 73, m.p. 265-269 °C, white crystalline solid; EI-MS m/z (rel. int. %): 337 (M⁺, 60), 159 (92), 280 (30), 83 (100), 110(65); ¹H NMR (DMSO-d₆, 300 MHz); δ 10.42 (s, ¹H, NH), 7.62 (d, J=8.4Hz, ¹H, Ar), 7.65 (bs, 1H, Ar), 7.55-7.51 (m, 2H, Ar), 7.16 (t, J=9.0 Hz, 2H, Ar), 7.33 (d, J=6.9Hz, 1H, Ar), 4.21 (s, 2H, CH₂).

2.6 Characterization by Spectroscopy

Electron impact mass spectra (EI-MS) were recorded using a MASPEC system, while field desorption mass spectrometry (FD-MS) and peak analysis were conducted on a Finnigan MAT 312 instrument. Caesium iodide (CsI) was employed as the internal reference for high-resolution mass determinations. One-dimensional ¹H NMR spectra were acquired in DMSO-d₆ using a Bruker Avance AM-300 MHz spectrometer. Chemical shifts (δ) are presented in ppm relative to tetramethylsilane (SiMe₄) as internal standard, with coupling constants (J) reported in hertz.

2.7 Compounds Detection by Chromatography

Chromatograms were taken on TLC plates and UV radiation was examined at 366 nm for fluorescent spots and 254 nm for fluorescence quenching spots.

2.8 Urease Inhibition Assay

To evaluate urease inhibition, 5 μ L of each synthesized compound was incubated at 30 °C for 15 minutes in a 96-well microplate, in the presence of 25 μ L of jack bean urease enzyme and 55 μ L of buffer solution containing 100 mM CH₄N₂O. Urease activity was quantified by measuring ammonia production using the indophenol-based colorimetric method, as described by Weatherburn. For color development, 45 μ L of C₆H₅OH reagent (1% w/v C₆H₅OH and 0.005% w/v Na₂ [Fe (CN)₅NO] · 2H₂O) was added to each well, followed by 70 μ L of alkaline reagent composed of 0.5% w/v NaOH and 0.1% available Cl from NaOCl. The reaction mixture was allowed to proceed and after 50 minutes, the absorbance was recorded at 630 nm using a microplate reader (Molecular Device, USA). Each assay was performed in triplicate, with a final reaction volume of 200 μ L. CH₄N₂S served as the standard inhibitor for urease [25]. The findings (change in absorbance per minute) were obtained using Soft Max Pro (Molecular Device, USA). A pH of 6.8 was used for all of the experiments. Inhibition percentages were calculated using the following formula:

$$100 - (\text{OD test well}/\text{OD control}) \times 100 \quad (1)$$

2.9 Docking analysis

Molecular docking was performed on the urease active site (PDB ID: 3LA4) using AutoDock Vina [26]. A grid box of dimensions 48 \times 44 \times 40 Å was applied along the x, y, and z axes, with the grid center set at coordinates: x = -39.950, y = -47.558, and z = 77.251. The docking simulations employed the Lamarckian Genetic Algorithm (LGA) for a total of 100 runs. Throughout the process, the ligands were treated as flexible, whereas the protein structure remained rigid. The

same docking parameters were used for all oxadiazole derivatives (7a–7h). The docking outcomes were analyzed and visualized using PyMOL and Discovery Studio Visualizer (DSV) 2021, and the web-based platform <https://proteins.plus>.

3 Result

3.1 Research Scheme

From an industrial, pharmacological, and agricultural standpoint, 1,3,4-oxadiazole is important. Several similar processes are used in a number of commercially available drugs for the betterment of human health. Information on the synthesis and biological evaluation of these substances derived from benzoic acid derivatives is widely available. According to the literature it is thought to create substituted 1,3,4-oxadiazole from $C_6H_5CONHNH_2$. A procedure for creating substituted 1,3,4-oxadiazoles is shown in Figure 1 below in order to fulfil the objectives of this study.

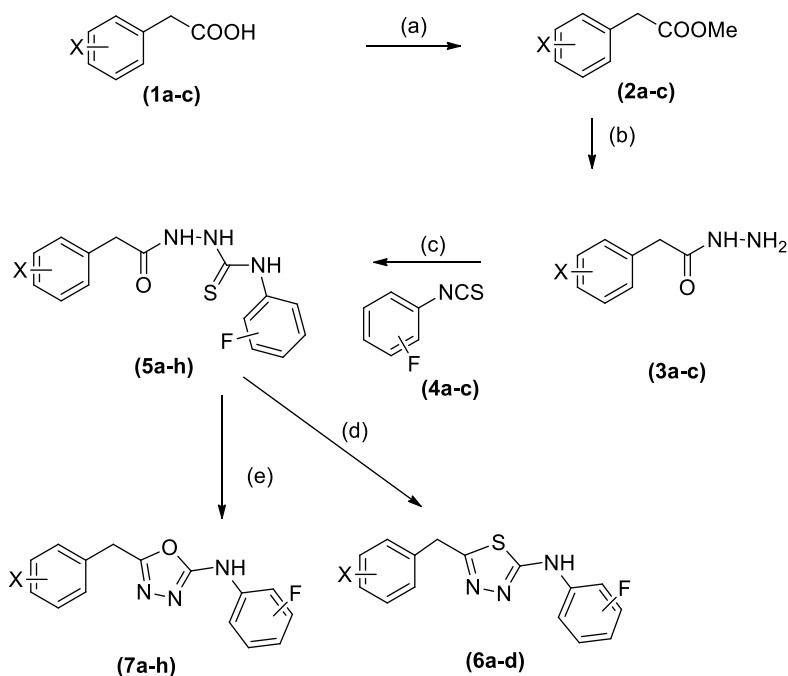


Figure 1 Oxadiazol synthesis research scheme.

3.2 Synthesis of Esters 2(a-c)

Using concentrated sulfuric acid (H_2SO_4) as a catalyst, the di-chlorophenyl acetic acids 1 (a-c) reacted with methanol to produce methyl esters 2(a-c). Figure 2 below shows the esterification of di-chlorophenyl acetic acid.

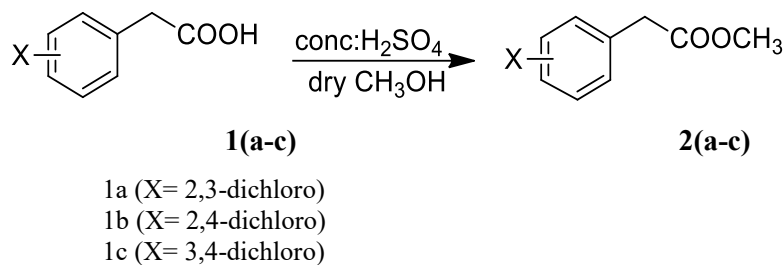


Figure 2 Esterification of di-chlorophenyl acetic acid.

The disappearance of the wide acid peak in the 2400-3200 cm^{-1} region is a characteristic of esters 2(a-c). The yield (%) of 1a, 1b, 1c was 88, 92 and 86 respectively. According to physical properties all were liquid in nature. The C=O of 2(a-c) was 1733, 1725 and 1730 cm^{-1} and C=C, 1571-1481, 1564-1478, 1555-1459 cm^{-1} respectively.

3.3 Synthesis of Hydrazides 3(a-c)

The following step was refluxing with hydrazine hydrate in methanol to convert the esters 2(a-c) of di-chlorophenyl acetic acids to their corresponding hydrazides 3(a-c). Aqueous ethanol was used to recrystallize the resulting hydrazides 3(a-c). Figure 3 shows the synthesis of hydrazides.

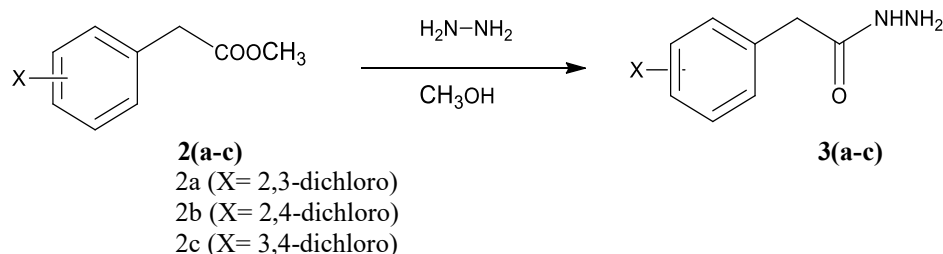


Figure 3 Hydrazides synthesis by treating esters with hydrazine.

The IR spectra of the hydrazide derivatives 3(a-c) exhibited a characteristic absorption band attributable to the stretching vibration of the primary amine group ($-\text{NH}_2$), accompanied by a shoulder, within the 3281–3293 cm^{-1} range. Additionally, a separate absorption band attributed to the secondary amino group (NH) was observed between 3029 and 3041 cm^{-1} . A strong absorption band observed between 1632 and 1641 cm^{-1} in the IR spectra was attributed to the carbonyl group of the amide linkage. Compounds 3(a-c) were obtained as white solids, with yields of 92%, 84%, and 86%, and melting points of 113–114 °C, 108–110 °C, and 123–126 °C, respectively.

3.4 Synthesis of 1,4-disubstituted thiosemicarbazides 5(a-h)

In the subsequent step, the target thiosemicarbazides 5(a–h) were synthesized by reacting the corresponding R–CO–NH–NH₂ 3(a–c) with fluorinated isothiocyanates 4(a–c) in CH₃OH. The synthetic pathway for thiosemicarbazides from hydrazides and isothiocyanates is illustrated in Figure 4.

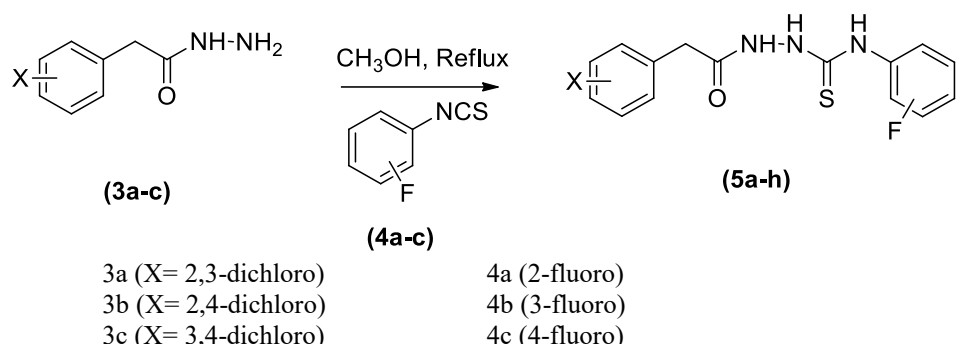


Figure 4 Synthesis of thiosemicarbazides from Hydrazides and isothiocyanates.

The successful synthesis of thiosemicarbazides 5(a–h) was verified through IR spectroscopy, which displayed characteristic carbonyl (C=O) stretching vibrations in the range of 1634–1678 cm^{–1} and thiocarbonyl (C=S) absorptions between 1236 and 1268 cm^{–1}. Additionally, three distinct bands corresponding to secondary N–H groups were observed within the 3148–3367 cm^{–1} region. Further confirmation was obtained from the ¹H NMR spectra, which exhibited downfield signals between 10.19 and 11.29 ppm, attributed to amide-type NH protons, while the NH protons related to thiourea moieties resonated between 9.52 and 10.22 ppm.

3.5 Synthesis of 1,3,4-oxadiazoles 7(a-h)

The synthesis of 1,3,4-oxadiazole derivatives commenced with the esterification of alcohols and carboxylic acids under acidic conditions to yield the corresponding esters. In the subsequent step, these esters were reacted with hydrazine hydrate to produce the respective hydrazides. The obtained hydrazides were then treated with isothiocyanates to form thiosemicarbazide intermediates. Cyclization of these thiosemicarbazides in the presence of mercuric acetate resulted in the formation of 1,3,4-oxadiazoles. Upon completion of each reaction, the mixtures were filtered, and the solvents were evaporated to isolate crystalline products from the filtrates. The synthetic pathway for oxadiazoles is illustrated in Figure 5.

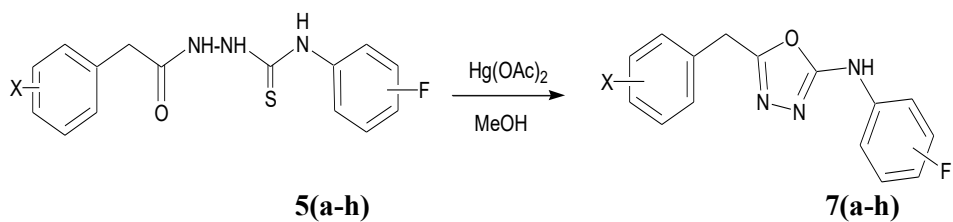


Figure 5 Oxadiazoles synthesis by the cyclization of thiosemicarbazides.

The formation of oxadiazoles 7(a–h) was confirmed through ^1H NMR spectroscopy, which showed a characteristic N–H proton resonance in the range of 10.20 to 10.69 ppm. The absence of signals corresponding to other N–H protons further supported the successful synthesis of the oxadiazole ring. Additional confirmation was provided by electron impact mass spectrometry (EIMS), which exhibited a molecular ion peak at m/z 337 with relative intensities ranging from 14% to 67%. The physical appearance of synthesized compound 7a was white crystalline solid, the %yield was 52, the melting point was 264–266 °C, while compound 7b was white solid, the %yield was 58, and the melting point was 271–273 °C. Similarly, compounds 7c, 7d, 7e, 7f, 7g, and 7h showed the following physical properties: %yield 64, 47, 59, 62, 67, and 73, respectively, while the melting points were 267–269, 259–262, 256–257, 277–279, 273–276, 265–269 °C, respectively. All compounds were white solid in shape, except 7f and 7h, which were white crystalline solid.

3.6 Urease Inhibition

Table 1 below summarizes the findings of the evaluation of the urease inhibitory ability of the oxadiazole compounds 7(a–h). Comparing these compounds to the standard inhibitor, thiourea, revealed a variety of inhibitory actions, from moderate to weak, according to the IC_{50} values.

Table 1 Urease inhibition by Oxadiazole compounds.

No	Compound	$\text{IC}_{50} \pm \text{SEM} [\mu\text{M}]$
1	7a	Not active
2	7b	342.6 ± 5.8
3	7c	284.6 ± 5.8
4	7d	161.6 ± 5.8
5	7e	453.6 ± 5.8
6	7f	Not active
7	7g	265.6 ± 5.8
8	7h	Not active
9	Thiourea (Std)	21.8 ± 1.51

Compounds (7d) and (7g) exhibited the most promising inhibitory activity, with IC_{50} values of $161.6 \pm 5.8 \mu\text{M}$ and $265.6 \pm 5.8 \mu\text{M}$, respectively. In contrast, compounds 7b, 7c, and 7e exhibited moderate inhibition, while compounds 7a, 7f, and 7h did not show any activity.

3.7 Molecular Docking Results

Of the candidate ligands, (7d) exhibited a significantly lower binding energy of -7.4 kcal/mol and its RMSD value was 1.573 Å. It was followed by ligand 7g with a binding energy of -7.2, 7b at -7.1, 7f at -6.7, 7e at -6.7, 7b at -6.6, 7a at -6.5 and 7h at -6.3 kcal/mol. The RMSD values exhibited by compounds 7a, 7b, 7c, 7e, 7f, 7g, and 7h were 1.277, 1.841, 1.294, 2.918, 1.898, 0.00, and 3.135 Å, respectively. The RMSD value of almost all compounds was smaller than 2 Å, except for 7e, which had an RMSD value of 2.918 Å, and 7h, which had an RMSD value of 3.135 Å, i.e., larger than 2 Å. Compounds 7e and 7h showed RMSD values above 2 Å (2.918 Å and 3.135 Å, respectively), suggesting that their binding within the active site may be flexible or unstable and that their position reliability is limited, because inadequate docking geometry or poor fitting are frequently indicated by RMSD values greater than 2 Å. In vitro, both medications showed negligible or no urease inhibition, which is in line with their less-than-ideal docking properties. This emphasizes that while high RMSD values would suggest molecules with weak or non-specific binding, persistent, low-RMSD conformations displayed strong hydrogen bonding (such as 7d interacting with His593) indicating biological activity. These limitations highlight the necessity of providing experimental validation for docking predictions.

Table 2 Molecular docking results.

No	Compounds	Affinity/ kcal/mol	RMSD/ Å	Hydrogen Bonding
1	7a	-6.5	1.277	His593
2	7b	-6.6	1.841	Gln649
3	7c	-7.1	1.294	His492, His593
4	7d	-7.4	1.573	His593
5	7e	6.7	2.918	-
6	7f	6.7	1.898	His593
7	7g	7.2	0.00	His593
8	7h	6.3	3.135	-

Several criteria help to determine the best-docked enzyme-ligand complex. The most important aspect is the binding energy of the docked enzyme-ligand complex. For compound 7a, hydrogen bonding was at His593, 7b at Gln649, while 7c showed two hydrogen bonding interactions, at His492 and His593, 7e

and 7h did not show any hydrogen bonding, 7f and 7g exhibited only one hydrogen bonding interaction, at His593. Based on the binding energy values and hydrogen bonding interactions obtained from the molecular docking studies, ligand 7d emerged as the most promising inhibitor of the urease active site, as depicted in Table 2 and illustrated in Figures 6, 7, 8 and 9.

The molecular docking study demonstrated a significant relationship between the binding affinity of the oxadiazole derivatives and their measured urease inhibitory effects. Compound 7d had the lowest binding energy (-7.4 kcal/mol) and the highest in vitro activity ($IC_{50} = 161.6 \pm 5.8 \mu M$). The hydrogen bond with His593, a crucial residue involved in the catalytic mechanism of urease, was one of the significant interactions observed in the 7d-urease complex. In order to stabilize the active site and coordinate the nickel ions needed for urea hydrolysis, His593 is crucial. The interaction between this and the proton transfer mechanism is probably disrupted by 7d's binding to His593, which lowers enzyme activity. Compound 7c's modest in vitro activity corresponds with its favorable binding affinity (-7.1 kcal/mol) and the hydrogen bonds it formed with both His492 and His593. On the other hand, compounds 7e and 7h, which showed no biological activity at all, had high RMSD values (2.918 Å and 3.135 Å, respectively) and were unable to establish hydrogen bonds with important catalytic residues, suggesting insufficient docking reliability. Even while molecules like 7g make hydrogen bonds with His593, the considerably reduced activity may be explained by their high binding energy (-7.2 kcal/mol) and potential conformational stiffness. Together, the data show that certain interactions, most notably hydrogen bonding with His593 as well as advantageous binding energy and spatial conformation, are necessary for this group of oxadiazole compounds to successfully inhibit urease.

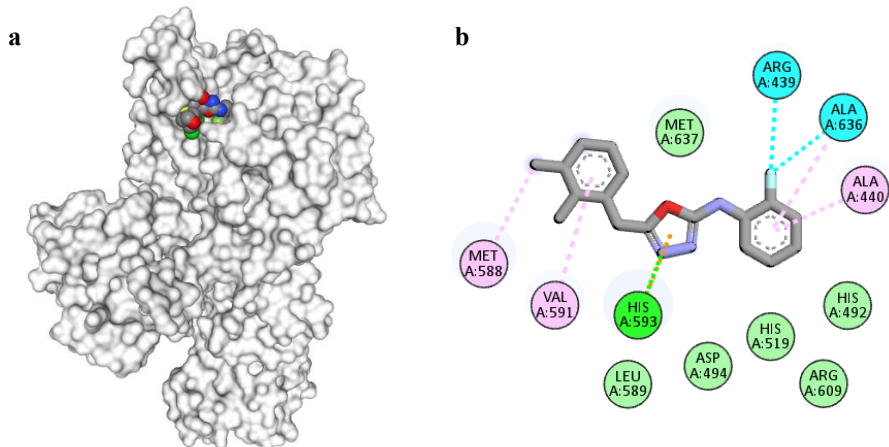


Figure 6 (a and b) Interactions of 7a with urease enzyme.

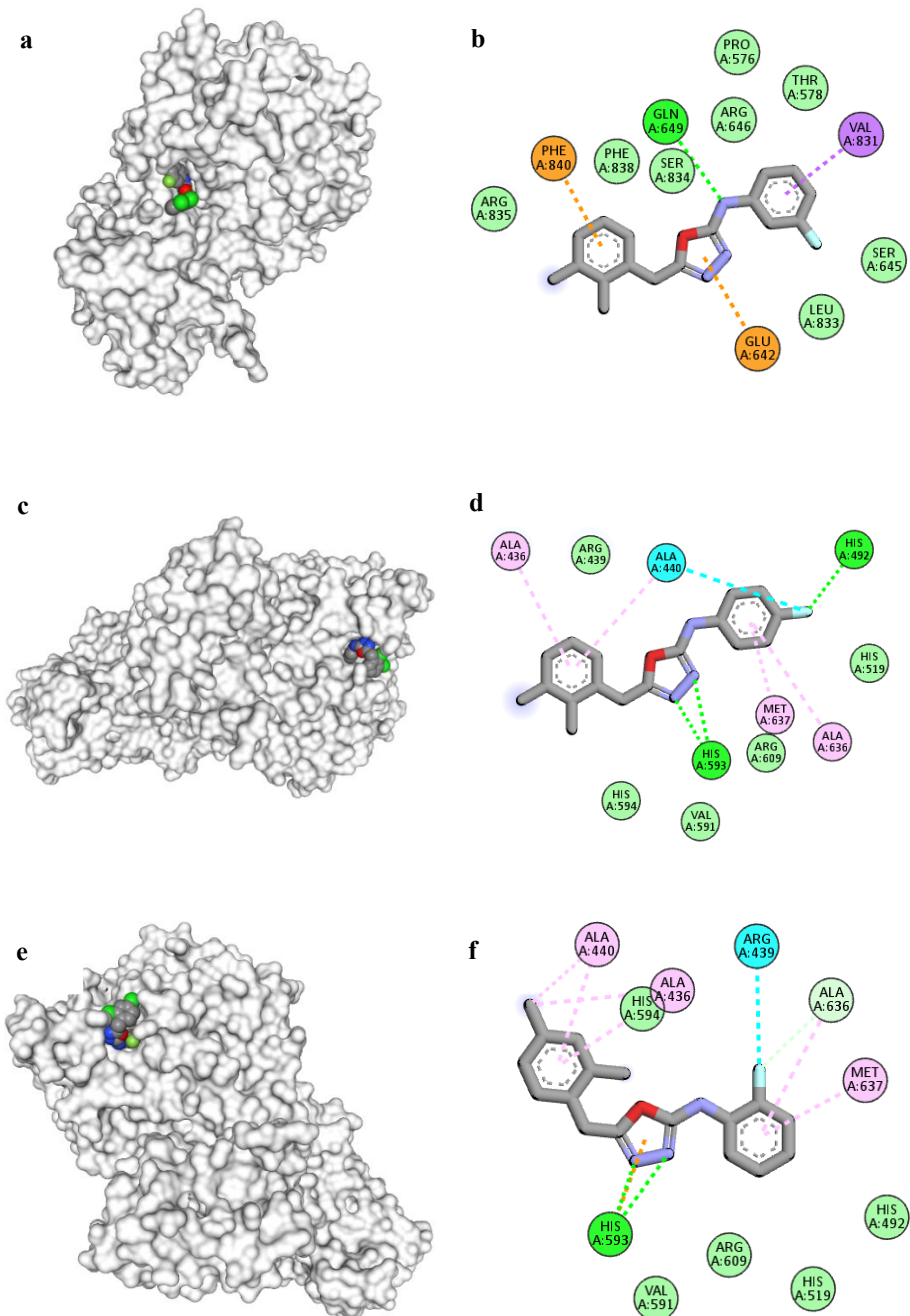


Figure 7 (a and b) 7b; (c and d) 7c; (e and f) 7d.

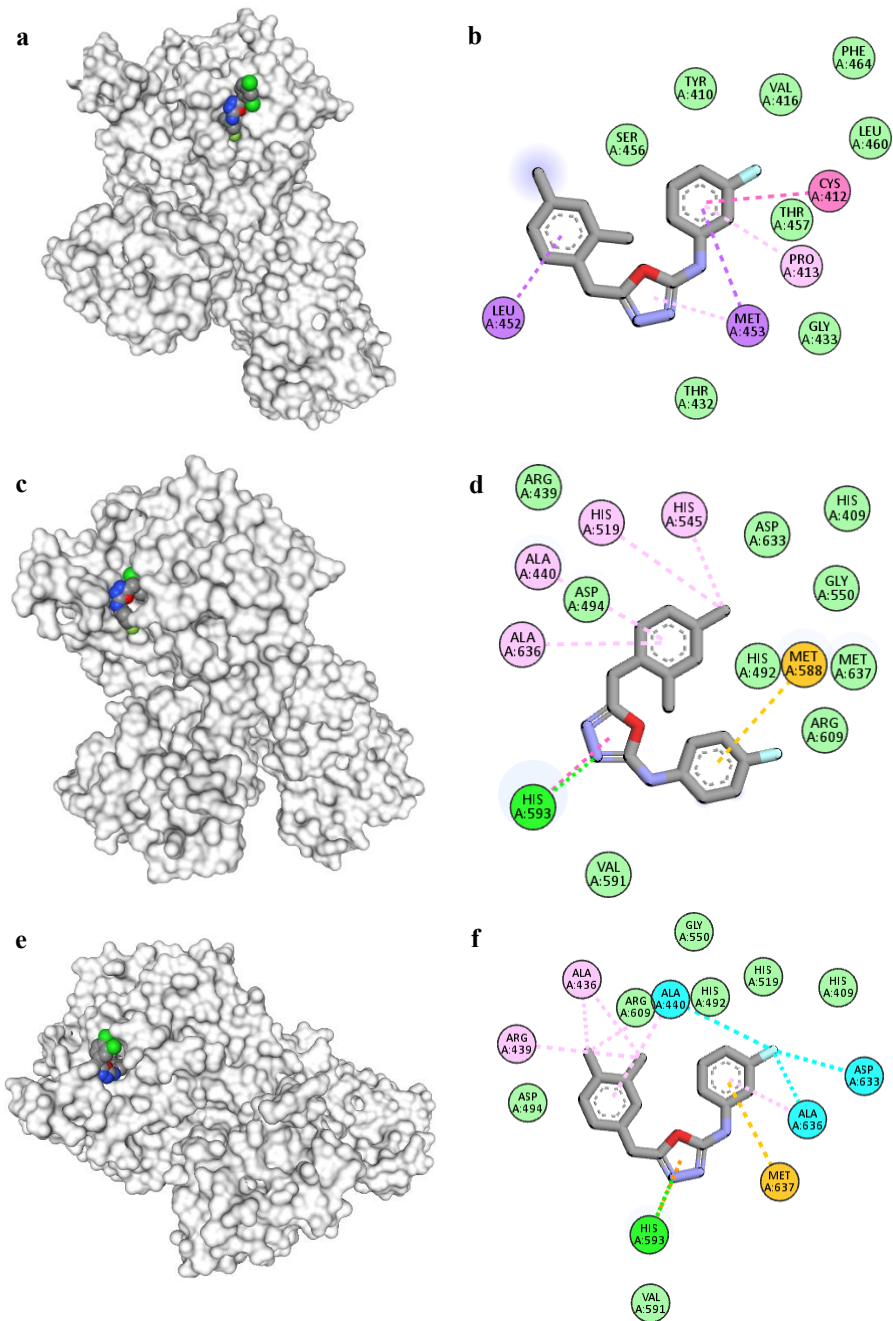


Figure 8 (a and b) 7e; (c and d) 7f; (e and f) 7g.

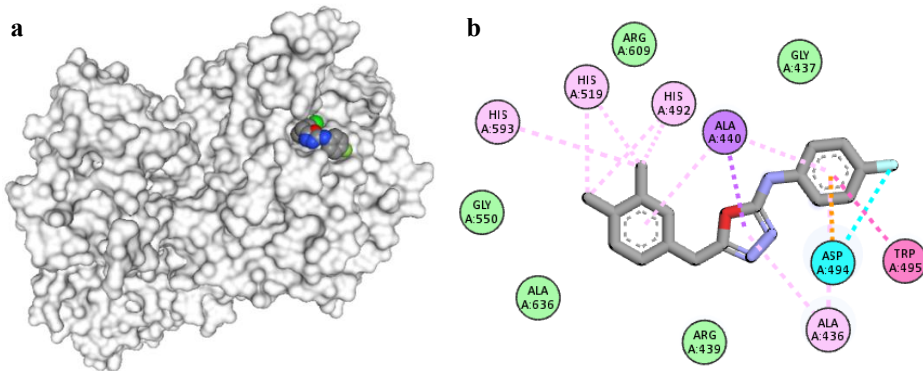


Figure 9 (a and b) The interactions of 7h with the enzyme.

Although ligands and the targeted enzyme may interact in a number of ways, conventional hydrogen bonding is the most common and efficient ligand-enzyme interaction. In addition to hydrogen bonding, the oxadiazole derivatives exhibit a variety of van der Waals interactions with urease. In the case of the most promising compound (7d), it exhibited van der Waals interactions at Ala436, Arg439, Ala440, His492, His519, Val591, His594, Arg609, Ala636, and Met637.

4 Discussion

Esterification is one of the important steps in oxadiazole synthesis [27]. Synthesis of hydrazides is a necessary step for the synthesis of oxadiazole [28]. When preparing heterocyclic compounds like oxadiazoles and thiadiazols, the thiosemicarbazides 5(a–h) serve as intermediates [29]. Using aqueous ethanol, the synthesized thiosemicarbazides 5(a–h) are recrystallized. An alternative synthetic approach involves the nucleophilic attack of acid hydrazide 2 on isothiocyanic acid, leading to the formation of the corresponding thiosemicarbazide derivative [30]. A variety of oxadiazole synthesis techniques have also been developed. For example, Hackler produced alkyl oxadiazole through heating 1-Acyl-2-ethoxymethylene hydrazine at room temperature [31]. Other investigations included the synthesis of 1,3,4-oxadiazole using pyrazole moiety and oxadiazole compounds replaced with amines [32] and 3,5-diaryl derivatives consisting of 1,2,4-oxadiazole groups linked by a pharmacophoric group at C₅ and a phenyl, benzyl, or 4-trifluoromethylphenyl group at C₃ [33]. The 1,3,4-oxadiazole scaffold is considered a privileged structure in medicinal chemistry due to its wide range of pharmacological properties. These compounds have great potential for therapeutic use, including anti-inflammatory, anti-cancer, anti-bacterial, and anti-viral and as a urease inhibitor [34]; their urease inhibition results from this study are described below.

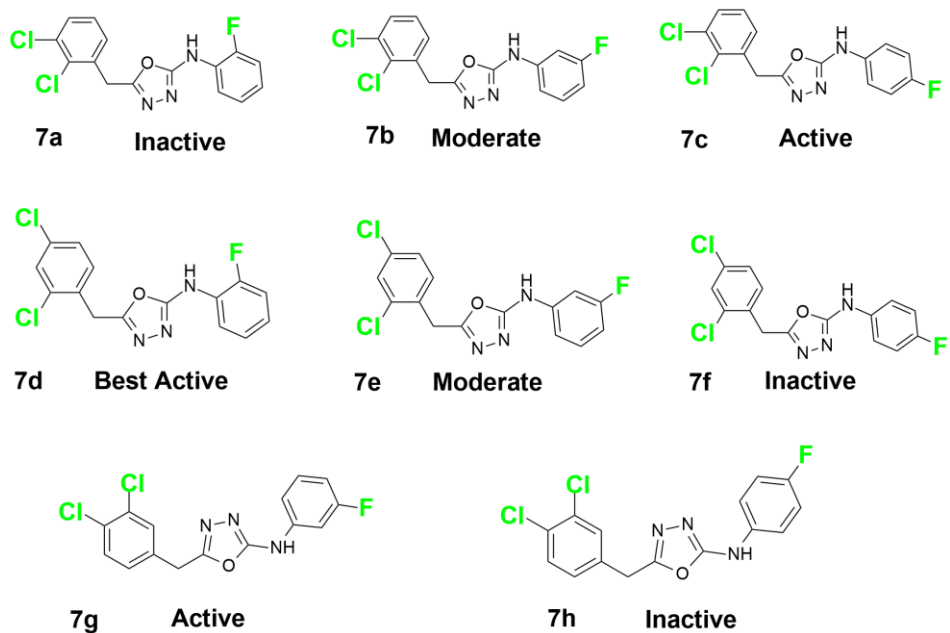


Figure 10 Structure activity relationship (SAR) of oxadiazole derivatives (7a-7h).

As can be seen in Figure 10, compound 7d exhibits the highest inhibition, which is because of the result of the fluorine substituent's electron-donating action at the ortho position [35]. This improves nitrogen's electronegativity and interactions with the urease enzyme by raising its charge density [36]. Furthermore, compound 7d has two chlorine groups that are further apart, which lessens steric hindrance [37]. However, because its fluorine substituent is at the meta position, where it does not have an electron-donating effect, 7e exhibits the least amount of inhibition [38]. It is important to note that these results are consistent with research on 1,3,4-oxadiazole derivatives that found molecules with methoxy groups at positions 2, 3, and 4 have potent urease inhibitory effects. This was explained by the methoxy groups' ability to donate electrons, which improved their interactions with the urease enzyme. On the other hand, derivatives with methoxy groups at the meta location showed less effective inhibitory effects, which is in line with this configuration's decreased capacity to donate electrons. [39].

Destructive halogen substitution techniques that significantly affect the structural and electrical properties of compounds 7a, 7f, and 7h may be the direct cause of their lack of urease inhibitory activities. Because of the 2,3-dichlorobenzyl moiety in compound 7a, the ortho and meta chlorine substituents experience

steric hindrance [21]. The steric hindrance forces the molecule into a distorted conformation that prevents ideal alignment inside the urease active site by disrupting the coplanarity of the oxadiazole core and the benzyl ring. According to the SAR study, urease inhibition is strongly influenced by the kind and location of substituents on the aryl and benzyl rings. On the other hand, active substances such as 7d have a 2-fluorophenyl moiety and a 2,4-dichlorobenzyl group. The benzyl ring's ortho- and para-chlorine atoms improve the molecule's electron-withdrawing properties, stabilize it via resonance, and probably strengthen hydrophobic contacts inside the urease binding site. By making the nearby amine more electrophilic and encouraging hydrogen bonding and appropriate orientation at the active site, the 2-fluoro substitution on the aryl ring improves binding even more [40].

In 7d, the ortho and para chlorine atoms efficiently remove electron density, stabilizing the oxadiazole ring structure due to its potential to form polar interactions with key residues in the active site of the target enzymes. This impact is attenuated in 7f and 7h, where the lack of chlorine at pivotal locations diminishes the molecule's capacity to participate in such interactions. Moreover, compounds 7f and 7h exhibit an ill-defined hydrophobic surface area owing to inadequate substitution, leading to diminished van der Waals interactions and reduced binding affinity. Furthermore, compound 7h lacks any critical functional group capable of functioning as a hydrogen bond donor or acceptor at the active site [41]. The structure is devoid of electrical polarization and conformational stiffness, both of which are critical for enzyme inhibition. The inactivity of 7a, 7f, and 7h can potentially and definitively be ascribed to the altered molecular shape, diminished electronic interaction potential, and the loss of hydrophobic and hydrogen bonding capabilities, all essential for efficient urease binding and inhibition.

Additionally, the literature reviewed on SAR trends in oxadiazole derivatives, revealed that electron-donating groups have slightly superior activity. The activity is influenced by the nature of the substituents, whether they are electron-withdrawing or electron-donating [42]. The nature, position, and number of substituents on the ring significantly influence the overall biological activity of the compounds [43]. When compared to the standard inhibitor thiourea ($IC_{50} = 21.8 \pm 1.51 \mu M$), all oxadiazole derivatives exhibited significantly lower urease inhibitory activity, indicating reduced potency relative to thiourea. Thiourea's superior efficacy highlights the need for further optimization of the oxadiazole scaffold to enhance its urease inhibitory activity [44]. The synthesized compounds exhibited moderate antibacterial activity against the tested bacterial strains. Theoretical experiments demonstrated that these compounds are non-toxic to both humans and animals [45]. Similarly, in another research, synthetic compounds had considerable activity; however, their antibacterial efficacy was

lower than the reference compound [46]. The observed differences in urease inhibition among the oxadiazole compounds can be attributed to their structural variations [47].

The presence of oxygen in the main skeleton, as opposed to sulfur, may contribute to the reduced inhibitory activity. Such structural differences are expected to modulate the interaction strength and binding behavior with the urease enzyme [48]. Among the candidate ligands, compound 7d made one hydrogen bond with an active pocket of urease at residue His593, confirmed by [49], and also showed several other interactions [50]. Several criteria help to determine the optimal docked enzyme-ligand complex. A key parameter in molecular docking studies is the binding energy of the enzyme-ligand complex, with the lowest binding energy generally indicating the most stable and favorable binding conformation [51]. In the current study, compound 7d exhibited the least binding energy and is considered to be the best-docked complex. Other research has emphasized the significance of binding energy, pointing out that it is more important than ligand-target protein interactions alone in choosing the best binding mode [52].

Another critical factor in molecular docking is the nature of the interactions between the compound and the receptor. In this context, the interaction of oxadiazole derivatives with the urease active site is the most important. A ligand is generally regarded as optimally docked if it occupies the same active site and interacts with the residues as the native ligand, indicating a favorable binding conformation [53]. Although ligands and the targeted enzyme may interact in a number of ways, conventional hydrogen bonding is the most common and efficient ligand-enzyme interaction. Van der Waals interactions, pi-cations, pi-anion, water hydrogen bonds, and other similar interactions are included in the second kind of interaction [54]. These interactions are similar with [55], which confirms that 7d is the best-docked complex with urease.

5 Conclusion

Using NMR and EI-MS analysis, a number of new 1,3,4-oxadiazole derivatives (7a-h) were created. Their structures were verified in this work. With an IC_{50} of $161.6 \pm 5.8 \mu M$, compound 7d showed the most urease inhibitory activity among them, whereas compounds 7a, 7f, and 7h showed no action. These findings were corroborated by molecular docking studies, which showed that 7d had a high binding affinity through hydrogen bonding interactions with His593 in the urease active site. According to these results, 7d) 5-(2,4-dichlorobenzyl)-N-(2-fluorophenyl)-1,3,4-oxadiazol-2-amine appears to be a potential lead chemical for urease inhibitor research. However, further research is required to fully understand its medicinal potential. To determine its safety and bioavailability, further research may involve pharmacokinetic analysis, toxicity profiling, and in

vivo tests. To improve inhibitory efficacy and selectivity, the oxadiazole scaffold's structural optimization may also be sought. These substances may also have more general biological properties, like anti-fungal, anti-bacterial, or anti-cancer properties.

Acknowledgements

Thanks to the whole staff of Department of Chemistry GPC Haripur Pakistan and Badan Riset dan Inovasi Nasional (BRIN) Indonesia for their unconditional support during whole research period.

References

- [1] Abid, O.U.R., Ayaz, M., Rehman, W., Mehdi, K., Ali, A., Wadood, A., Rahim, F., Sultan, A., Ghufran, M., Mir, S. & Qureshi, M.T., *Synthesis, Enzyme Inhibition, and Molecular Docking Studies of Hydrazones from Dichlorophenylacetic Acids*, Journal of the Chinese Chemical Society, **63**(12), pp. 1015–1021, 2016.
- [2] Mazzei, L., Musiani, F. & Ciurli, S., *Urease*, RSC Metallobiology, **2017**(10), pp. 60–97, 2017.
- [3] Takeuchi, T., *On the Occurrence of Urease in Higher Plants*, Journal of the College of Agriculture, **1**, pp. 1–14, 1909.
- [4] Jabri, E. & Andrew, P., *Structures of the Klebsiella aerogenes Urease Apoenzyme and Two Active-site Mutants*, Biochemistry, **35**(33), pp. 10616–10626, 1996.
- [5] Balasubramanian, A. & Ponnuraj, K., *Crystal Structure of the First Plant Urease from Jack Bean: 83 Years of Journey from its First Crystal to Molecular Structure*, Journal of Molecular Biology, **400**(3), pp. 274–283, 2010.
- [6] Mazzei, L., Musiani, F., Zambelli, B., Benini, S., Cianci, M. & Ciurli, S., *Urease: Structure, Function, Catalysis, and Inhibition*, Ureases, **2024**, pp. 165–208, 2024.
- [7] Yang, W., Feng, Q., Peng, Z. & Wang, G., *An Overview on the Synthetic Urease Inhibitors with Structure-activity Relationship and Molecular Docking*, European Journal of Medicinal Chemistry, **234**, 2022.
- [8] Kumar, S. & Kayastha, A. M., *Plant Ureases: Biochemistry, Structure, Physiological Functions, Role of Urease Inhibitors, and Urease Applications in Industry*, Ureases, **2024**, pp. 99–117, 2024.
- [9] Mazzei, L., Musiani, F. & Ciurli, S., *Urease*, RSC Metallobiology, **2017**(10), pp. 60–97, 2017.
- [10] Konieczna, I., Żarnowiec, P., Kwinkowski, M., Kolesińska, B., Frączyk, J., Kamiński, Z. & Kaca, W., *Bacterial Urease and its Role in Long-Lasting Human Diseases*, Current Protein & Peptide Science, **13**(8), pp. 789, 2012.

- [11] Zaib, S., Younas, M.T., Zaraei, S.O., Khan, I., Anbar, H.S. & El-Gamal, M.I., *Discovery of Urease Inhibitory Effect of Sulfamate Derivatives: Biological and Computational Studies*, Bioorganic Chemistry, **119**, 2022.
- [12] Song, W.Q., Liu, M.L., Li, S.Y. & Xiao, Z.P., *Recent Efforts in the Discovery of Urease Inhibitor Identifications*, Current Topics in Medicinal Chemistry, **22**(2), pp. 95–107, 2021.
- [13] Marahatta, A. & Ware, R.E., *Hydroxyurea: Analytical Techniques and Quantitative Analysis*, Blood Cells, Molecules, and Diseases, **67**, pp. 135–142, 2017.
- [14] Keogan, D.M., Twamley, B., Fitzgerald-Hughes, D. & Griffith, D.M., *Novel Class of Bi(III) Hydroxamate Complexes: Synthesis, Urease Inhibitory Activity and Activity Against H. pylori*, Dalton Transactions, **45**(27), pp. 11008–11014, 2016.
- [15] Bouchareb, F. & Berredjem, M., *Recent Progress in the Synthesis of Phosphoramidate and Phosphonamide Derivatives: A Review*, Phosphorus, Sulfur, and Silicon and the Related Elements, **197**(7), pp. 711–731, 2022.
- [16] Ahmed, N., Mehdi, K., Abid, R., Khan, S., Zikri, A. & Helianti, I., *Synthesis, in Vitro Activity, and Computational Evaluation of Novel Thiadiazole Derivatives as Potent Urease Inhibitors*, Results in Chemistry, **16**, 2025.
- [17] Masood, A., Khan, M.A., Bhat, M.A., Awan, B., Hanif, R., Raza, A., Khaliq, S., Ahmed, J. & Ullah, F., *Exploring Biological Activities of Novel Schiff Bases Derived from Amlodipine and in Silico Molecular Modeling Studies*, Future Medicinal Chemistry, **16**(22), pp. 2383–2394, 2024.
- [18] Ridwansyah, M., Abid, O.-ur-R., Rehman, W., Ilfan, F., Hamzah, S., Badshah, K.D., Ahmed, N., Ahmed, J., Ali, A. & Mehdi, K., *Characterization of Metallic Nanoparticles Synthesized via Green Synthesis from Viola odorata and their Application in Azo-dye Biodegradation: A Circular Economy Approach*, Current Research in Green and Sustainable Chemistry, **9**, 2024.
- [19] Boros, E., Dyson, P.J. & Gasser, G., *Classification of Metal-Based Drugs according to Their Mechanisms of Action*, Chem, **6**(1), pp. 41–60, 2020.
- [20] Hakimullah, Hussain, R., Khan, S., Rehman, W., Ullah, Z., Khan, Y., Rashid, M.U., Iqbal, T., Aziz, T., Alharbi, M. & Alshammari, A., *Exploring Target Site Interactions of 1,3,4-Oxadiazole/1,3,4-thiadiazole Derivatives: Synthesis, Characterization in Vitro Anti-urease and in Silico Molecular Docking Studies*, Journal of Molecular Structure, **1320**, 2025.
- [21] Hanif, M., Shoaib, K., Saleem, M., Rama, N.H., Zaib, S. & Iqbal, J., *Synthesis, Urease Inhibition, Antioxidant, Antibacterial, and Molecular Docking Studies of 1,3,4-Oxadiazole Derivatives*, International Scholarly Research Notices, **2012**(1), 2012.
- [22] Heena, Sharma, D., Om, H. & Rana, R., *Highly Twisted 1,3,4-oxadiazole*

based Hybrid Fluorescent Organic Materials: Synthesis, Characterization, Density Functional Theory Calculations, and Optoelectronic Study, Journal of Heterocyclic Chemistry, **61**(9), pp. 1417–1425, 2024.

- [23] Kwatra, A., Author, C. & Negi, B., *A Review of Recent Progress on the Anticancer Activity of Heterocyclic Compounds*, SynOpen, **8**(03), pp. 185–210, 2024.
- [24] Luczynski, M. & Kudelko, A., *Synthesis and Biological Activity of 1,3,4-Oxadiazoles Used in Medicine and Agriculture*, Applied Sciences, **12**(8), 2022.
- [25] Khan, S., Ullah, H., Rahim, F., Hussain, R., Khan, Y., Khan, M.S., Iqbal, R., Ali, B. & Albeshr, M.F., *Synthesis, Biological Evaluation and Molecular Docking Study of Pyrimidine based Thiazolidinone Derivatives as Potential Anti-urease and Anti-cancer Agents*, Journal of Saudi Chemical Society, **27**(4), 2023.
- [26] Morris, G.M., Ruth, H., Lindstrom, W., Sanner, M.F., Belew, R.K., Goodsell, D.S. & Olson, A.J., *AutoDock4 and AutoDockTools4: Automated Docking with Selective Receptor Flexibility*, Journal of Computational Chemistry, **30**(16), pp. 2785–2791, 2009.
- [27] Khormi, A.Y., El-sayed, R., Farghaly, T.A., Shaaban, M.R. & Farag, A.M., *An Exhaustive Compilation on the Synthesis of Heterocycles Pendant on the Fatty Acid Alkyl Chains*, Current Organic Synthesis, **20**(4), pp. 395–457, 2022.
- [28] Du, J., Su, Q., Pan, Y.M. & Ablajan, K., *I2-promoted One-pot Synthesis of 1,3,4-oxadiazoles from Aroyl Hydrazides and Methyl/ethyl Acetate*, Tetrahedron, **167**, 2024.
- [29] Othman, A.A., Kihel, M. & Amara, S., *1,3,4-oxadiazole, 1,3,4-thiadiazole and 1,2,4-triazole Derivatives as Potential Antibacterial Agents*, Arabian Journal of Chemistry, **12**(7), pp. 1660–1675, 2019.
- [30] Kalyani, M., Sireesha, S.M., Reddy, G.D. & Padmavathi, V., *Facile Synthesis of Pyrimidine Substituted-1,3,4-oxadiazole, 1,3,4-thiadiazole and 1,2,4-triazole Derivatives and their Antimicrobial Activity Correlated with Molecular Docking Studies*, Journal of Molecular Structure, **1312**, 2024.
- [31] Ainsworth, C. & Hackler, R.E., *AlkyI-1,3,4-oxadiazoles*, Journal of Organic Chemistry, **31**(10), pp. 3442–3444, 1966.
- [32] Sultana, R., Ali, A., Rana, M., Ahmad, I., Kamthan, M., Nouman, N., Mehandi, R. & Rahisuddin, *Synthesis of Oxadiazole Derivatives: Antibacterial, DNA Binding and in Silico Molecular Modelling Approaches*, Journal of Molecular Structure, **1318**, 2024.
- [33] Ayoub, M.S., Ghanem, M., Abdel-Hamid, H., Abu-Serie, M.M., Masoud, A., Ghareeb, D.A., Hawsawi, M.B., Sonousi, A. & Kassab, A.E., *New 1,2,4-oxadiazole Derivatives as Potential Multifunctional Agents for the Treatment of Alzheimer's Disease: Design, Synthesis, and Biological*

Evaluation, BMC Chemistry, **18**(1), pp. 1–15, 2024.

- [34] Salim, H. A. & Saoud, S. A., *A Review of Modern Methods of Synthesis 1, 3, 4-Oxadiazole as a Bioactive Compounds*, Wasit Journal for Pure Science, **2**(4), pp. 237-253, 2023.
- [35] Alzahrani, A.Y.A., Ullah, H., Bhat, M.A., Rahim, F., Al-Wesabi, E.O. & Alanazi, T.Y.A., *Design, Synthesis, in Vitro Acetylcholinesterase, Butyrylcholinesterase Activities, and in Silico Molecular Docking Study of Oxindole-oxadiazole Hybrid Analogues*, Journal of Molecular Structure, **1299**, 2024.
- [36] Khan, A., Elhenawy, A.A., Rehman, M.U., Alam, M., Alam, A., Rehman, N.U. & Ibrahim, M., *Synthesis of Novel 2-mercapto-1,3,4-oxadiazole Derivatives as Potent Urease Inhibitors: In Vitro and in Silico Investigations*, Journal of Molecular Structure, **1312**, 2024.
- [37] Khan, S., Iqbal, T., Hussain, R., Khan, Y., Fiaz, Z., Rahim, F. & Darwish, H.W., *Synthesis, Characterizations, Anti-Diabetic and Molecular Modeling Approaches of Hybrid Indole-Oxadiazole Linked Thiazolidinone Derivatives*, Pharmaceuticals, **17**(11), 2024.
- [38] Salauddin, Zaidi, S.A.A., Ubaid, M., Shamim, S., Naim, M.J., Khanna, S. & Alam, O., *Parkinson's Disease: A Progressive Neurodegenerative Disorder and Structure-Activity Relationship of MAO Inhibitor Scaffolds as an Important Therapeutic Regimen*, CNS & Neurological Disorders - Drug Targets, **24**, 2024.
- [39] Omar, A.Z., Elhag, M., Mohamed, A.K., Abd-Elmoneam, A.A., Mostafa, M.A. & Sadek, M.M.E., *Furan-oxadiazole Hybrids as Promising Antioxidants: Synthesis, Characterization, ADME and Molecular Docking Studies on Peroxiredoxin-2*, Journal of Molecular Structure, **1314**, 2024.
- [40] Bhat, R.M., Hegde, V., Budagumpi, S., Adimule, V. & Keri, R.S., *Benzimidazole-Oxadiazole Hybrids—Development in Medicinal Chemistry: An Overview*, Chemical Biology & Drug Design, **104**(2), 2024.
- [41] Kumar, A. & Bhatia, R., *Recent Advancements in Anticancer Activities of 1,2,4-Oxadiazole Conjugates*, JOJ Public Health, **6**(5), pp. 1-5, 2022.
- [42] Wieczorkiewicz, P.A., Krygowski, T.M. & Szatylowicz, H., *Substituent Effects and Electron Delocalization in Five-membered N-heterocycles*, Physical Chemistry Chemical Physics, **26**(28), pp. 19398–19410, 2024.
- [43] Janowska, S., Stefańska, J., Khylyuk, D. & Wujec, M., *The Importance of Substituent Position for Antibacterial Activity in the Group of Thiosemicarbazide Derivatives*, Molecules, **29**(6), 2024.
- [44] El-Masry, R.M., Kadry, H.H., Taher, A.T. & Abou-Seri, S.M., *Comparative Study of the Synthetic Approaches and Biological Activities of the Bioisosteres of 1,3,4-Oxadiazoles and 1,3,4-Thiadiazoles over the Past Decade*, Molecules, **27**(9), 2022.
- [45] Hamdan, I.A.A. & Tomma, J.H., *Synthesis, Characterization and Antimicrobial Evaluation for New Esters Derivatives Containing Two 1, 3,*

4-Oxadiazole Units, Iraqi Journal of Science, **65**(4), pp. 1800–1812, 2024.

[46] Gandhi, B., Jhansi, M., Deshpande, S.S., Vinay, T., Misra, S. & Kaki, S.S., *Design, Synthesis and Biological Activity of Novel Oxadiazole Containing Monoacylglycerols as Potential Bioactive Lipids*, Journal of Molecular Structure, **1284**, 2023.

[47] Maz, T.G., Caliskan, H.B., Capan, I., Caliskan, B., Özçelik, B. & Banoglu, E., *Design, Synthesis and Evaluation of Aryl-Tailored Oxadiazole-thiones as New Urease Inhibitors*, ChemistrySelect, **8**(8), 2023.

[48] Akhtar, T., Hameed, S., Khan, K.M., Khan, A. & Choudhary, M.I., *Design, Synthesis, and Urease Inhibition Studies of Some 1,3,4-oxadiazoles and 1,2,4-triazoles Derived from Mandelic Acid*, Journal of Enzyme Inhibition and Medicinal Chemistry, **25**(4), pp. 572–576, 2010.

[49] Zhang, W., Wang, H., Ding, C., Lei, Y., Yin, C., Wang, R., Yang, Q., Wu, T. & Zhang, M., *Bioactivity and Computational Studies on the Induction of Urease Inhibition by Three Cu(II) Complexes with a Fluorinated Schiff Base and Different Secondary Ligands*, Inorganic Chemistry Communications, **159**, 2024.

[50] Wang, H., Guo, P., Zhou, Y., Yin, C., Lei, Y., Wang, R., Wang, Y., Wu, T. & Zong, Z., *Urease Inhibition Studies of Two Cu(II) Complexes with an ONO Tridentate Schiff Base and Two Different Secondary Ligands: An Experimental, DFT, Molecular Docking and Molecular Dynamics Study*, Journal of Molecular Structure, **1321**, pp. 140093, 2025.

[51] Ahmed, N., Raharjo, S., Swasono, R.T. & Raharjo, T.J., *The Antibacterial Peptides (AMPs) Originated from Tryptic Hydrolysis of Naja Sumatrana Venom Fractionated Using Cation Exchange Chromatography*, Rasayan Journal of Chemistry, **15**(4), pp. 2642–2653, 2022.

[52] Adelin, T. & Dwinna A., *Molecular Docking of Curcumin and Its Analogue on Cyclooxygenase-2 Enzyme*, Jurnal Medika Veterinaria, **7**(1), 2013.

[53] Kakkassery, J.T., Raphael, V.P., Johnson, R. & K, V.T., *In Vitro Antibacterial and in Silico Docking Studies of Two Schiff Bases on Staphylococcus aureus and its Target Proteins*, Future Journal of Pharmaceutical Sciences, **7**(78), pp. 1-9 2021.

[54] Sharma, M., Farhat, N., Khan, A. U., Khan, F. H. & Mahmood, R., *Studies on the interaction of 2,4-dibromophenol with human hemoglobin using multi-spectroscopic, molecular docking and molecular dynamics techniques*, Journal of Biomolecular Structure and Dynamics, **42**(21), pp.11762-11772, 2024.

[55] Farooq, U., Khan, S., Naz, S., Wani, T. A., Bukhari, S. M., Aborode, A. T., Shahzad, S. A. & Zargar, S., *Three New Acrylic Acid Derivatives from Achillea millefolium as Potential Inhibitors of Urease from Jack Bean and α -Glucosidase from Saccharomyces cerevisiae*, Molecules, **27**(15), 2022.